Silicon Etching in XeF_2 Environment

R. Knizikevičius*
Department of Physics, Kaunas University of Technology, 73 K. Donelaičio St., LT-44029 Kaunas, Lithuania

(Received February 9, 2011; revised version March 11, 2013; in final form May 1, 2013)

Enhancement of silicon etching rate in XeF_2 environment is considered by a proposed model, which includes processes of adsorption, activation, chemical reactions, relaxation, desorption, and sputtering. The enhancement of silicon etching rate is explained by considering hydrocarbon molecules from background gas contamination in the vacuum chamber, and assuming that hydrocarbon radicals enhance the etching rate. The composition of the adsorbed layer during silicon etching in XeF_2 environment is calculated. It is found that hydrocarbon radicals intensify reaction of XeF_2 molecules with Si atoms on the surface and that this changes the kinetics of the etching rate. Using the obtained theoretical results the difference in kinetics of the etching rates of first and subsequent run is explained.

DOI: 10.12693/APhysPolA.124.137
PACS: 81.65.Cf, 82.35.Gh, 82.65.+r

1. Introduction

XeF_2 is a solid white crystal at atmospheric pressure and room temperature, which sublimates at pressure about 500 Pa. Materials commonly used in integrated circuit manufacture, such as photoresist, aluminium, and silicon dioxide, are not attacked by this dry etchant [1]. XeF_2 is the only commercially available xenon derivative. A characteristic feature of this reagent is that it behaves as a fluorinating agent in the gas phase or under irradiation. Silicon etching in XeF_2 environment represents an attractive alternative to study the reactive ion etching process [2–6]. In integrated circuit manufacture, it is required to eliminate several types of wafer contamination which may influence the next step in the etching process and the final reliability of the device. As dimensions of features are decreasing, wafer contamination becomes more and more persistent. The main form of contamination consists of traces of metal, sputtered from walls or electrodes, which are deposited on wafer surface [7]. Depending on the type of reactor and materials used for electrodes, traces of Ca, Fe, Zn, Cr, Mn, Ni, Cu, and K in the range from 0.01 to 0.4 ML may be found on the wafer after etching. Even after extensive cleaning some of these contaminants remain on the surface [8]. Another source of contamination consists of solutions used for photoresist development [9, 10]. The development of sensitive equipment to detect small traces of contamination follows the increased concern about contaminants. However, the influence of activated polymer on the etching rate is little investigated.

In previous works [11, 12], silicon etching in XeF_2 environment was considered. It was found that ion bombardment intensifies adsorption of XeF_2 molecules on the surface and subsequent reaction of adsorbed XeF_2 molecules with Si atoms. The polymer formed on the surface slows down the etching rate at later stages of the etching process [13, 14]. In this work, the kinetics of the ion-beam-assisted etching rate of Si in XeF_2 environment is investigated. The influence of hydrocarbon radicals on the chemical reactions taking place on the Si surface is determined. Thin vapour-deposited Si films are etched in XeF_2 environment [15]. The etching process is performed in a diffusion-pumped high-vacuum system. It is important to note that photoresist masks are not used in the experiment. XeF_2 molecules emanated from the Knudsen beam at the flow rate 2.0×10^{15} molecules/s. The beam is directed to the film being etched and produced the effective pressure at the surface about 10^{-1} Pa at temperature 300 K. Ar^+ ions are directed to the grounded Si film at normal incidence and bombarded the surface with the energy 450 eV. The etching rate is measured using quartz crystal microbalances. It is found that the hydrocarbon radicals in the adsorbed layer intensify reaction of XeF_2 molecules with Si atoms and that this changes the kinetics of the etching rate. The difference in kinetics of the etching rates of first and subsequent run is explained.

2. Model

During Si etching in XeF_2 environment, competition between etching and polymerization processes takes place. The etching process does not proceed by continuous removal of the outermost Si layer, but by the formation of a fairly thick, disordered reaction layer containing SiF, SiF_2, and SiF_3 species [16–18]. Under certain conditions, the trapped SiF_4 molecules are also observed. The reaction layer is formed when F atoms, produced during dissociative adsorption of XeF_2 molecules, diffuse in the adsorbed layer [19, 20] and near-surface region [4]. The etching process in the presence of polymerizing species is driven by ion bombardment. Polymerization prevails at low energy of incident ions (≈ 10 eV). Meanwhile, at higher energy of incident ions (> 100 eV), the etching process becomes pronounced.

*e-mail: Rimantas.Knizikevicius@ktu.lt

The model is proposed to explain experimentally observed enhancement of etching rate and difference in kinetics of the etching rates of first and subsequent run during Si etching in XeF_2 environment [15, 21]. A mechanism of the enhanced Si etching rate, which is based on the activation of adsorbed hydrocarbon molecules, is used in the model. The mechanism is following: (1) adsorbed hydrocarbon molecules are slowly activated, usually by creating radicals; (2) hydrocarbon radicals in the polymer film enhance the reaction of XeF_2 molecules with Si atoms. Small amounts of hydrocarbon molecules are present in the vacuum chamber. They originate from an oil used in the vacuum pump. XeF_2 and C_xH_y molecules from the gas phase adsorb on the surface

$$\mathrm{XeF_2(g)} \rightarrow \mathrm{XeF_2(a)}, \tag{1a}$$

$$\mathrm{C}_x\mathrm{H}_y\mathrm{(g)} \rightarrow \mathrm{C}_x\mathrm{H}_y\mathrm{(a)}. \tag{1b}$$

These processes are characterized by adsorption frequencies $\kappa_1 = \alpha_1 N(\mathrm{XeF_2})$ and $\kappa_2 = \alpha_2 N(\mathrm{C}_x\mathrm{H}_y)$, where α_i is the sticking coefficient of i-th type species and $N(i)$ is the concentration of i-th type species in the gas phase. Adsorbed C_xH_y molecules are activated by incident Ar^+ ions

$$\mathrm{C}_x\mathrm{H}_y\mathrm{(a)} \xrightarrow{\mathrm{Ar}^+} \mathrm{AP}, \tag{2}$$

where AP is the hydrocarbon radicals in the polymer film. The hydrocarbon radicals have dangling bonds and chemisorb species in the adsorbed layer. The activation process is characterized by activation frequency

$$G = gI_0/C, \tag{3}$$

where g is the activation constant, I_0 is the ion flux, and C is the surface concentration of Si atoms ($C = 1.36 \times 10^{19}\ \mathrm{m}^{-2}$). The activated polymer relaxes: $\mathrm{AP} \rightarrow \mathrm{C}_x\mathrm{H}_y\mathrm{(a)}$. This process is characterized by relaxation frequency $R = \tau_\mathrm{r}^{-1}$, where τ_r is the mean relaxation time.

The main reactions, taking place in the adsorbed layer, are the following:

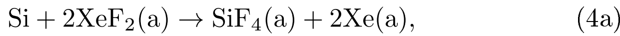

$$\mathrm{Si} + 2\mathrm{XeF_2(a)} \rightarrow \mathrm{SiF_4(a)} + 2\mathrm{Xe(a)}, \tag{4a}$$

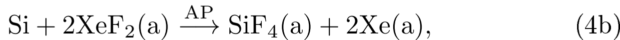

$$\mathrm{Si} + 2\mathrm{XeF_2(a)} \xrightarrow{\mathrm{AP}} \mathrm{SiF_4(a)} + 2\mathrm{Xe(a)}, \tag{4b}$$

$$2\mathrm{C}_x\mathrm{H}_y\mathrm{(a)} \xrightarrow{\mathrm{AP}} \mathrm{P}, \tag{4c}$$

$$\mathrm{P} + \mathrm{C_xH_y(a)} \xrightarrow{\mathrm{AP}} \mathrm{P}. \tag{4d}$$

It is important to note that these reactions do not represent elementary steps. Rather, they are composite reactions that embody the most important kinetics parameters. The reactions are characterized by reaction rate constants k_1, k_2, k_3, and k_4, respectively. Let us assume that polymer formed during reactions, defined by Eqs. (4c) and (4d), is much slower activated than adsorbed C_xH_y molecules. The components of the adsorbed layer desorb and are sputtered by incident ions. The removal frequency of i-th adsorbed layer component consists of desorption and sputtering frequencies

$$\omega_i = \tau_{i,\mathrm{d}}^{-1} + \tau_{i,\mathrm{s}}^{-1} = \nu_0 \exp\left(-E_{i,\mathrm{d}}/kT\right) + Y_i I_0/C, \tag{5}$$

where τ_i is the mean lifetime of i-th component, ν_0 is the oscillation frequency of atoms in the solid, $E_{i,\mathrm{d}}$ is the desorption activation energy of i-th type species, k is the Boltzmann constant, T is the temperature, and Y_i is the sputtering yield of i-th component. Sputtering of activated polymer, polymer, and Si atoms is characterized by sputtering frequencies, $\omega_i = \omega_{i,\mathrm{s}}$. Ion bombardment increases the removal of SiF_x radicals [22, 23]. However, this phenomenon does not change the etching rate and is not included in the model.

Components, present in the gas phase and produced during reactions on the surface, are included in the adsorbed layer of one-monolayer thickness. Six components exist in the adsorbed layer: XeF_2, SiF_4, Xe, C_xH_y, AP, and P, with relative concentrations $c_1 = [\mathrm{XeF_2}]/C$, $c_2 = [\mathrm{SiF_4}]/C$, $c_3 = [\mathrm{Xe}]/C$, $c_4 = [\mathrm{C}_x\mathrm{H}_y]/C$, $c_5 = [\mathrm{AP}]/C$, and $c_6 = [\mathrm{P}]/C$. The relative surface concentration of Si atoms is equal to $c_7 = 1$. The following system of equations includes rate expressions of processes mentioned earlier and describes the kinetics of component concentrations in the adsorbed layer:

$$\begin{cases} \frac{\mathrm{d}c_1}{\mathrm{d}t} = \beta\kappa_1 - 2k_1c_1^2 - 2k_2c_1^2c_5 - \omega_1c_1, \\ \frac{\mathrm{d}c_2}{\mathrm{d}t} = k_1c_1^2 + k_2c_1^2c_5 - \omega_2c_2, \\ \frac{\mathrm{d}c_3}{\mathrm{d}t} = 2k_1c_1^2 + 2k_2c_1^2c_5 - \omega_3c_3, \\ \frac{\mathrm{d}c_4}{\mathrm{d}t} = \beta\kappa_2 - Gc_4 - 2k_3c_4^2c_5 - k_4c_4c_5c_6 \\ \quad + Rc_5 - \omega_4c_4, \\ \frac{\mathrm{d}c_5}{\mathrm{d}t} = Gc_4 - Rc_5 - \omega_5c_5, \\ \frac{\mathrm{d}c_6}{\mathrm{d}t} = k_3c_4^2c_5 + k_4c_4c_5c_6 - \omega_6c_6, \end{cases} \tag{6}$$

where $\beta = 1 - \Theta$ is the fraction of the surface not covered with adsorbate and $\Theta = \sum_{i=1}^{6} c_i$ is the surface coverage. The etching rate is proportional to the removal rate of formed SiF_4 molecules and Si atoms

$$V = h_0\left(\omega_2c_2 + \omega_7c_7\right), \tag{7}$$

where $h_0 = 2.72$ Å is the thickness of a monolayer.

3. Results and discussion

The experimentally measured kinetics of silicon etching rate in XeF_2 environment [15] is used to determine the influence of activated polymer on the enhancement of etching rate. The experimental and theoretical kinetics of silicon etching rate are shown in Fig. 1. The values of reaction rate constants and frequencies, found by extrapolation from experimental data, are presented in Table. It is observed that ion bombardment increases adsorption of XeF_2 molecules and C_xH_y molecules. The obtained theoretical results are in agreement with experimental measurements [24]. The removal frequencies of XeF_2, SiF_4 molecules, and Xe atoms increase in the presence of ion bombardment. The sputter yield of SiF_x radicals increases with respect to Si atoms due to a decrease in binding energy. Large yields of SiF_x radicals exhibiting a collision cascade-type energy distribution are observed by time-of-flight experiments [25]. The mean lifetime of SiF_4 molecules in the adsorbed layer in presence of ion bombardment is equal to 19.4 ms. The experimentally measured value is about 40 ms [23]. The difference between

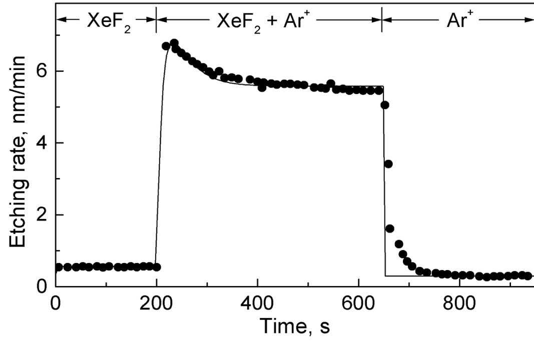

Fig. 1. Experimental [15] (points) and theoretical (curve) kinetics of silicon etching rate in XeF_2 environment.

TABLE

The values of reaction rate constants and frequencies, found by extrapolation from experimental data.

Reaction rate constant or frequency $[s^{-1}]$	$t < 200$ s	$200\ s \leq t < 650$ s	$t \geq 650$ s
κ_1	70	100	0
κ_2	2.4	3.0	3.0
G	0	0.027	0.027
R	0	0	0
k_1	0.35	0.35	0.35
k_2	0	80	80
k_3	0	0.50	0.50
k_4	0	0.50	0.50
ω_1	0.15	51.5	51.5
ω_2	0.15	51.5	51.5
ω_3	0.15	51.5	51.5
ω_4	0.40	0.40	0.40
ω_5	0	0.014	0.014
ω_6	0	0.40	0.40
ω_7	0	0.018	0.018

theoretical and experimental mean lifetimes is caused by ion bombardment parameters. Ion bombardment driven transport of reaction products through the reaction layer is reaction-rate limiting step at low ion flux [26].

The kinetics of concentrations of adsorbed layer components during silicon etching in XeF_2 environment, calculated using Eq. (6), are shown in Fig. 2. It is observed that, in the absence of ion bombardment, XeF_2, SiF_4 molecules, and Xe atoms prevail in the adsorbed layer. In the presence of ion bombardment, concentrations of these species vanish due to increased removal frequencies. Concentrations of C_xH_y molecules and activated polymer increase. The activated polymer intensifies reaction of XeF_2 molecules with Si atoms and enhances the etching rate. At later stages of the etching process, surface coverage by activated polymer increase and the etching rate starts to decrease.

The difference in kinetics of the etching rates of first and subsequent run is observed experimentally [21, 27].

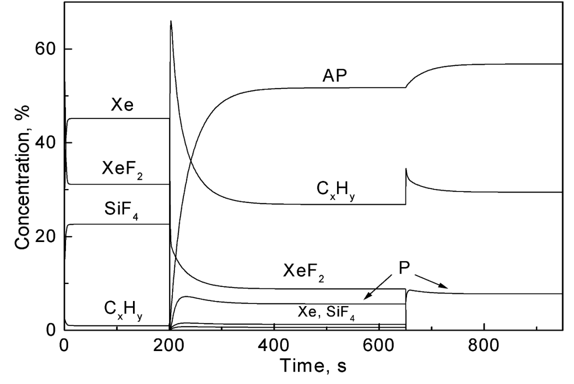

Fig. 2. The kinetics of concentrations of adsorbed layer components.

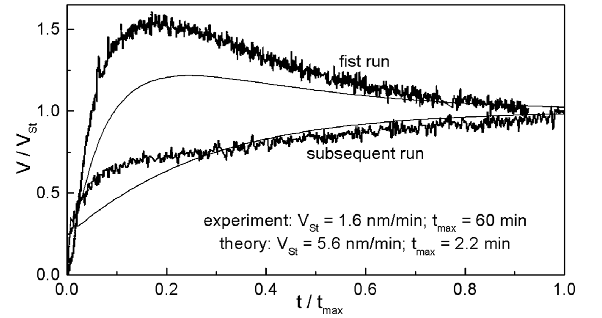

Fig. 3. Experimental [21] (dashed curves) and theoretical (curves) kinetics of silicon etching rates of first and subsequent run.

It is found that subsequent run starts on a less reactive surface. The proposed model explains the difference in kinetics of the etching rates. It is assumed that C_xH_y molecules present in the adsorbed layer are activated before the subsequent run (C_xH_y molecules are activated thermally at zero incident ion energy). The experimental [21] and theoretical kinetics of silicon etching rate are shown in Fig. 3. During the experiment the steady-state etching rate is reached later because of the absence of ion bombardment.

The kinetic chain length of the polymer is the average number of monomers added to each polymerizing radical during polymerization. The kinetic chain length is defined as the ratio of the number of propagation steps to the number of initiation steps:

$$l = \frac{k_4 c_6}{k_3 c_4}. \tag{8}$$

The dependence of kinetic chain length on time is shown in Fig. 4. The kinetic chain length increases due to increased adsorption of C_xH_y molecules when the flow of XeF_2 molecules is switched off. The monomer conversion is calculated using the Carothers equation

$$p = 1 - \frac{1}{X_n}, \tag{9}$$

where $X_n = l + 1$ is the number-average degree of poly-

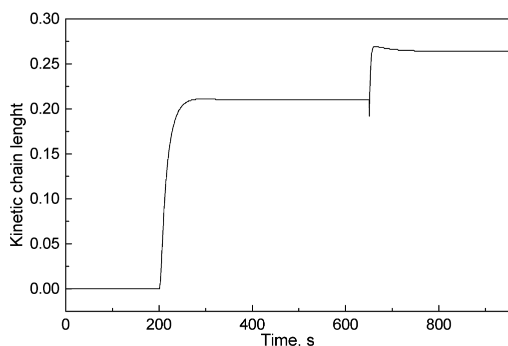

Fig. 4. The dependence of kinetic chain length on time.

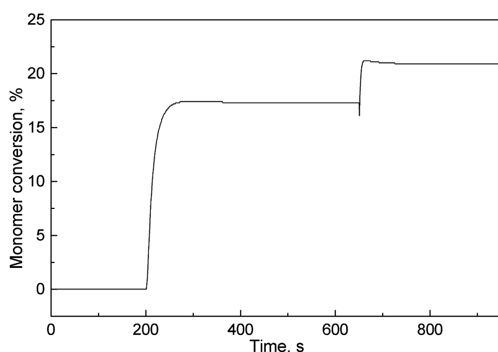

Fig. 5. The kinetics of monomer conversion.

merization. The kinetics of monomer conversion is shown in Fig. 5. The monomer conversion increases due to increased adsorption of C_xH_y molecules. The kinetic chain length and the monomer conversion increase with the increase of concentration of activated polymer.

4. Conclusions

1. The activated polymer intensifies reaction of XeF_2 molecules with Si atoms on the surface and enhances the etching rate at energy of incident ions 450 eV. The increased surface coverage by activated polymer slightly decreases the etching rate at later stages of the etching process.

2. The difference in kinetics of the etching rates of first and subsequent run is due to the activation of C_xH_y molecules present in the adsorbed layer.

References

[1] J. Jeon, A.H. Ma, K. Khosraviani, A.M. Leung, in: *2007 Canadian Conf. Electrical and Computer Engineering, Vancouver*, Institute of Electrical and Electronics Engineers, Vancouver 2007, p. 963.

[2] V.K. Brel, N.S. Pirkuliev, N.S. Zefirov, *Russ. Chem. Rev.* **70**, 231 (2001).

[3] B. Bahreyni, C. Shafai, *J. Vac. Sci. Technol. A* **20**, 1850 (2002).

[4] H.F. Winters, D.B. Graves, D. Humbird, S. Tougaard, *J. Vac. Sci. Technol. A* **25**, 96 (2007).

[5] R.C. Hefty, J.R. Holt, M.R. Tate, S.T. Ceyer, *J. Chem. Phys.* **129**, 214701 (2008).

[6] R.C. Hefty, J.R. Holt, M.R. Tate, S.T. Ceyer, *J. Chem. Phys.* **130**, 164714 (2009).

[7] P.G.M. Sebel, L.J.F. Hermans, H.C.W. Beijerinck, *J. Vac. Sci. Technol. A* **17**, 755 (1999).

[8] P. Verdonck, C.M. Hasenack, R.D. Mansano, *J. Vac. Sci. Technol. B* **14**, 538 (1996).

[9] T. Makino, H. Nakamura, M. Asano, *J. Electrochem. Soc.* **128**, 103 (1981).

[10] L.K. White, J. Maa, *Appl. Phys. Lett.* **46**, 1050 (1985).

[11] R. Knizikevičius, A. Galdikas, *Lith. J. Phys.* **41**, 55 (2001).

[12] R. Knizikevičius, *Lith. J. Phys.* **43**, 135 (2003).

[13] R. Knizikevičius, *Vacuum* **81**, 230 (2006).

[14] R. Knizikevičius, *Microelectron. Eng.* **86**, 55 (2009).

[15] J.W. Coburn, H.F. Winters, *J. Appl. Phys.* **50**, 3189 (1979).

[16] D. Humbird, D.B. Graves, *J. Appl. Phys.* **96**, 791 (2004).

[17] D. Humbird, D.B. Graves, *J. Vac. Sci. Technol. A* **23**, 31 (2005).

[18] F. Gou, A.W. Kleyn, M.A. Gleeson, *Int. Rev. Phys. Chem.* **27**, 229 (2008).

[19] Y. Fujikawa, S. Kuwano, K.S. Nakayama, T. Nagao, J.T. Sadovski, R.Z. Bahktizin, T. Sakurai, Y. Asari, J. Nara, T. Ohno, *J. Chem. Phys.* **129**, 234710 (2008).

[20] Y. Asari, J. Nara, T. Ohno, *Surf. Sci.* **605**, 225 (2011).

[21] M.J.M. Vugts, M.F.A. Eurlings, L.J.F. Hermans, H.C.W. Beijerinck, *J. Vac. Sci. Technol. A* **14**, 2780 (1996).

[22] J.L. Mauer, J.S. Logan, L.B. Zielinski, G.C. Schwartz, *J. Vac. Sci. Technol.* **15**, 1734 (1978).

[23] G.J.P. Joosten, M.J.M. Vugts, H.J. Spruijt, H.A.J. Senhorst, H.C.W. Beijerinck, *J. Vac. Sci. Technol. A* **12**, 636 (1994).

[24] P.G.M. Sebel, L.J.F. Hermans, H.C.W. Beijerinck, *J. Vac. Sci. Technol. A* **18**, 2759 (2000).

[25] R.A. Haring, A. Haring, F.W. Saris, A.E. de Vries, *Appl. Phys. Lett.* **41**, 174 (1982).

[26] R. Knizikevičius, *Vacuum* **79**, 119 (2005).

[27] H.F. Winters, D. Haarer, *Phys. Rev. B* **36**, 6613 (1987).